

Experiments towards high-energy electron cooling

A.V. Fedotov¹, B. Gålnander², V.N. Litvinenko¹, T. Lofnes², A. Sidorin³, A. Smirnov³, V. Ziemann²

¹*Brookhaven National Laboratory, Upton, New York 11973*

²*The Svedberg Laboratory, S-75121 Uppsala, Sweden*

³*JINR, Dubna, Russia*

High-energy electron cooling, presently considered as an essential tool for several applications in high-energy and nuclear physics, requires an accurate description of the friction force which ions experience by passing through an electron beam. Present low-energy electron coolers can be used for a detailed study of the friction force. In addition, parameters of a low-energy cooler can be chosen in a manner, to reproduce regimes expected in future high-energy operation. Here, we report a set of dedicated experiments aimed towards a detailed study of the magnetized friction force.

Electron cooling of heavy particle beams is used in a wide range of experiments in elementary-particle physics, nuclear physics, atomic physics, and other applications. High-energy electron cooling (with relativistic parameter $\gamma \gg 1$) can open new possibilities in particle physics by producing high quality high-density beams in colliders. However, the cooling times at high energy are much longer than the cooling times in present low-energy coolers. As a result, typical order of magnitude estimate of cooling times for high-energy becomes not practical. An accurate estimate of the cooling times requires the detailed description of Coulomb collisions in a strong magnetic field, a topic which is of great interest both for accelerator and plasma physics communities. Coulomb collisions in a magnetic field can be described by the friction force which ions experience when moving through the electron beam of the cooler. In this paper we discuss measurements based on the longitudinal friction force (the component parallel to the magnetic field and the direction of propagation of the electron beam) for protons at the injection energy of 48 MeV.

The friction force as a function of various parameters has been measured before (see, for example, [1, 2] and references therein). However, a detailed quantitative comparison with theory was never an issue since the cooling times in low-energy coolers are very short making an order of magnitude description satisfactory. In fact, experimental data, which can be found in review reports, and their comparison with theory presented on a double logarithmic scale was considered sufficient [3]. In order to have an accurate description at a level needed for high-energy cooling predictions, the measurements should be specifically aimed towards such a goal. This requires not just a high precision of the measurements but also a well-controlled experiment where all needed parameters are systematically measured. It also requires careful optimization of the cooling process and minimization of various effects which may obscure comparison with theory. For example, if the electron and ion beam are not perfectly aligned the values of the friction force are significantly reduced, so that even the non-magnetized friction force description may be very close to the mea-

surements [4]. One needs to carefully minimize such effects in order for the measurements to be suitable for a detailed comparison with the magnetized theory. The experiments reported in this paper were specifically aimed towards getting such a data needed for accurate validation of theories, which necessarily meant a well-controlled experiments with careful optimization of cooling, as well as control of various effects which one encounters when the cooler parameters are significantly changed from the standard operational settings. In addition, we found out that a complete characterization of the proton distribution during the measurements is needed since convoluting of the single-particle formulas with the proton distribution function is essential in order to have a detailed comparison with the data which is measured for a distribution of particles. In our experiments, for each measurement of the friction force curve, parameters of the proton distribution were carefully recorded.

The experiments reported in this paper were performed as part of a collaboration between BNL and European laboratories working on high-energy cooling for the RHIC-II [5] and FAIR projects [6]. The measurements, which were done at CELSIUS [7] in December 2004 and March 2005, can be characterized as follows: a) High-precision measurement of the longitudinal friction force. b) Condition of a well-controlled experiment were satisfied. c) A complete characterization of ion distribution was made for each set of the measurements. For standard operational parameters of the cooler the force was measured: 1) for various currents of electron beam; 2) for different alignment angles between electron and ion beams; 3) for different strength of the magnetic field errors in cooling solenoid. In addition, standard parameters of the cooler were altered in order to explore some effects, understanding of which is essential for high-energy magnetized cooling: 4) description of Intrabeam Scattering (IBS) for non-Gaussian distributions which may appear as a result of slow cooling process; 5) various regimes of magnetization. Details of the last two experiments are provided later in the text.

For low relative velocities between ions and electrons the longitudinal magnetized friction force increases lin-

early with velocity, reaching its maximum near the longitudinal velocity spread of the electron beam. There are several effects which can contribute to the longitudinal velocity spread, often referred to as "effective velocity". For relative velocities higher than the "effective velocity" the force has a non-linear dependence. In the linear region, the simplest way of measurement is the phase-shift method. It uses a bunched ion beam and is based on measuring the phase difference between the RF system and the ion beam, resulting from the competition of the weak RF voltage and the longitudinal friction force. Using an accurate phase discriminator, one can determine the cooling force acting on the ion of charge (Ze) via

$$F_{\parallel} = \frac{ZeU_{rf} \sin \Delta\phi_s}{L_c}, \quad (1)$$

where L_c is the length of cooling solenoid, U_{rf} is the rf amplitude, and $\Delta\phi_s$ is the equilibrium phase difference between the ion beam and the RF cavity. Typically, the relative velocity difference is introduced by changing the energy of the electron beam. However, changing the electron acceleration voltage is usually done with a rather large voltage step, which does not allow an accurate mapping near the force maximum. On the other hand, since this method employs bunched beams, changing the energy of the ion beam by changing the frequency of the RF cavity is more accurate. In our experiments, changing the RF frequency by a few Hz (1 Hz of 1129 kHz) resulted in a very fine step in relative velocity. A similar technique was used successfully before, for example at IUCF [8]. A high precision in the measurements was obtained due to a combination of the two effects: 1) a technique, described above, and 2) accurate measurements of the phase difference using the phase discriminator. An estimate of all types of errors in our measurements is summarized in Table 1. In Figures, reported in this paper, we present the raw data measurements of the relative phase shift $\Delta\phi$ vs. the frequency change Δf for proton at 48 MeV, which are converted to the plots of F_{\parallel} vs. v_{\parallel} , respectively, using Eq. 1 and Eq. 2 and parameters in Table 1.

$$v_{\parallel} = \frac{\beta c \Delta f}{\eta_p f}, \quad (2)$$

where c is the velocity of light, β is the relativistic factor, η_p is the slip factor, Δf and f are the frequency shift and rf frequency respectively. Using different calibrating techniques to measure the RF amplitude, the uncertainty was minimized to $\pm 7\%$. The total estimated relative error of measurements of the longitudinal friction force is $\pm 12\%$ (see Table 1), which has sufficient accuracy for detailed benchmarking with theories.

In all experiments reported in this paper, the main goal was collecting data with an uncertainty of just a few percent (see Table 1). In addition, the location of the force maximum was accurately recorded using the technique

TABLE I: Parameters and estimate of errors

	Value	Error	Comment
C	81.76m	$\pm 0.1 \%$	circumference
η_p	0.783	$\pm 0.5 \%$	from optics
Δf		$\pm 0.01 \%$	frequency generator
v_{\parallel}		$\pm 0.5 \%$	total error
U_{rf}	10.2V	$\pm 7 \%$	measurement
$\Delta\phi$		$\pm 1 \%$	phase discriminator
L_c	2.50m	$\pm 10 \%$	cooler length
F_{\parallel}		$\pm 12 \%$	total error

described below. The derivative of the force changes its sign near the force maximum (see Fig. 1), resulting in large synchrotron oscillations for the relative velocities in the non-linear part of the force [8]. For each measurement the onset of such oscillations was recorded which provided an accurate information about the relative velocity corresponding to the force maximum. This information is of critical importance when one wants to compare measured force with theory. Also, in all the experiments, the

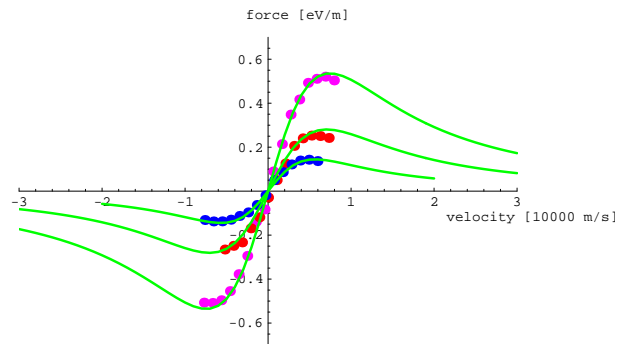


FIG. 1: Friction force for three currents of electron beam. Measured data: 250 (pink dots), 100 (red dots) and 50 (blue color) mA ($B=0.1$ T). Green lines: fitted curves.

proton and electron beam were first perfectly aligned by minimizing the spread of the beam profiles on the H^0 detector located outside of the cooling section.

In the first experiment, the force was measured for various currents of the electron beam. An example of the measured force for the electron currents of 250, 100 and 50 mA ($B = 0.1$ T) is shown on Fig. 1. In the analysis of the experimental data we realized that in order to determine an accurate numerical coefficient in the expression of the single-particle force by comparison with the measured data, one needs to convolute the single-particle expressions over the proton momentum distribution. Such detailed comparison of formulas with the data will be presented in a separate report. For the data shown in Fig.1, measured parameters of the proton distribution are the following: transverse FWHM

$\approx 2\text{mm}$, rms $dp/p = 5e-5$ ($I_e = 250\text{ mA}$); FWHM $\approx 2\text{mm}$, rms $dp/p = 6e-5$ ($I_e = 100\text{ mA}$); FWHM $\approx 2.5\text{mm}$, rms $dp/p = 5.5e-5$ ($I_e = 50\text{ mA}$). The beta functions in the cooler and in the magnesium jet location (transverse profiles) can be taken 10 and 10.5m, respectively.

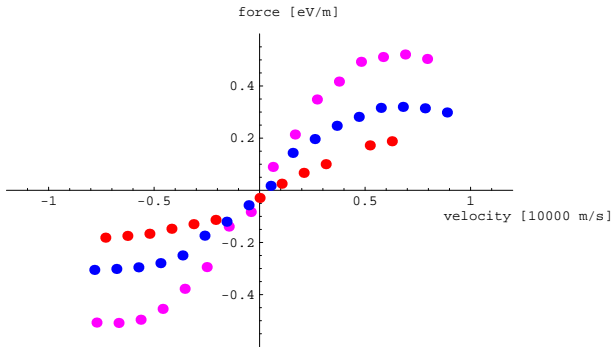


FIG. 2: Measured friction force for horizontal tilts: 0 (pink), 0.4 (blue), 0.8 (red) mrad ($B = 0.1\text{ T}$, $I_e = 250\text{ mA}$).

In a second experiment we explored the effective velocity dependence on the alignment angle between the ion and electron beam. A tilt angle introduces a significant contribution to the transverse component of the relative velocity in a controlled way. The friction force was systematically measured for several horizontal and vertical tilt angles from 0.2 to 0.8 mrad in both negative and positive directions. The angle values were calibrated both with Beam Position Monitors (BPMs) and an H^0 monitor. An example of the measured force for three tilt angles in positive horizontal directions is shown in Fig. 2.

The goal of the third experiment was to study simultaneous effects due to the electron cooling and IBS before the equilibrium parameters are reached. In a typical low-energy cooler, the electron cooling is so fast that one observes rapid cooling of the ion beam profile as a whole. At high-energy with much slower cooling speed, one may observe a slow formation of a dense beam core with pronounced beam tails. For the accurate description of the luminosity gain for such distributions it becomes critical to have an accurate treatment of intrabeam scattering. Recently, some models were developed in an attempt to describe this process [9–11]. In this experiment, the strength of the electron cooling was specifically reduced in order to capture such transient profiles of the ion beam. In the longitudinal direction, the recorded bunch profile shows the formation of a core with a subsequent cooling of large amplitudes, as shown in Fig. 3. The formation of non-Gaussian distributions are clearly observed. In the transverse direction, the transient evolution of horizontal profiles was recorded with the magnesium jet profile monitor, which also showed formation of a dense core. This data will be used to improve models for the IBS for the distributions evolving under the electron cooling.

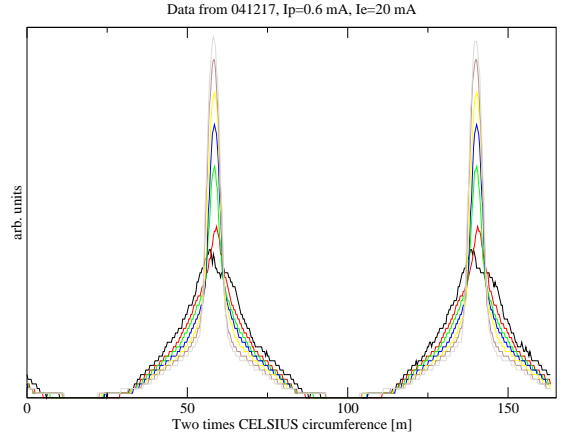


FIG. 3: Longitudinal profiles for $I_e = 20\text{ mA}$ and $I_p = 0.6\text{ mA}$, shown with the time step of 0.75 s.

The fourth experiment was devoted to studying various degrees of magnetization. In a strong magnetic field, the electron dynamics in the transverse direction is effectively frozen, which together with the flattened velocity distribution of the electrons results in very fast cooling. As a result, for the magnetized component of the friction force there is only a weak logarithmic dependence on both the magnetic field and transverse velocity spread of electrons which enters in the friction force expression through the Larmor radius under the Coulomb logarithm, using the description based on binary collisions. However, if the maximum impact parameter in magnetized collisions is not large compared to the Larmor circle one may encounter a strong non-logarithmic dependence on both the magnetic field and transverse velocity of electrons if the parameterization of the friction force [12] is used:

$$F = C \frac{4\pi n_e Z^2 e^4}{m_e} \frac{V}{(V^2 + \Delta_{eff}^2)^{3/2}} \ln(\rho_{max}/\rho_L + 1), \quad (3)$$

where V is the relative ion velocity, Δ_{eff} is the longitudinal effective velocity spread of electrons, ρ_{max} is the maximum impact parameter in binary ion-electron collisions, ρ_L is the Larmor radius, n_e and m_e is the density and mass of electrons, and C is some numeric coefficient. Here, we do not discuss the exact numeric coefficient C in Eq. 3 since it is exactly the goal of the first experiment, which will be the subject of a dedicated report. For the purpose of the experiment discussed in this section we are concerned only with the parametric dependence on the magnetic field in Eq. 3, which enters through the Larmor radius $\rho_L = m_e \Delta_{e\perp} / eB$, where $\Delta_{e\perp}$ is the transverse rms velocity spread of the electron distribution. If the maximum impact parameter in magnetized collisions is not large compared to the Larmor circle there is a possibility

of a non-logarithmic dependence on both the magnetic field and the transverse velocity of electrons. In such a case with $\alpha = \rho_{max}/r_L < 1$ one can replace $\ln(\alpha + 1)$ by α . As a result, the force has a linear dependence on the magnetic field and the transverse velocity of electrons which leads to a strong reduction in its absolute value. The idea of the experiment was to measure the friction force for various values of α . The values of α were controlled by changing the current of the electron beam (which changes ρ_{max}) and strength of the magnetic field (which changes r_L). As an example, the measured force for the values $\alpha = 1.3, 1.0, 0.9, 0.8$ (calculated based on measured effective velocity) with $I_e = 300$ mA is shown in Fig. 4. Measurements were done for other currents of the electron beam and other values of α as well.

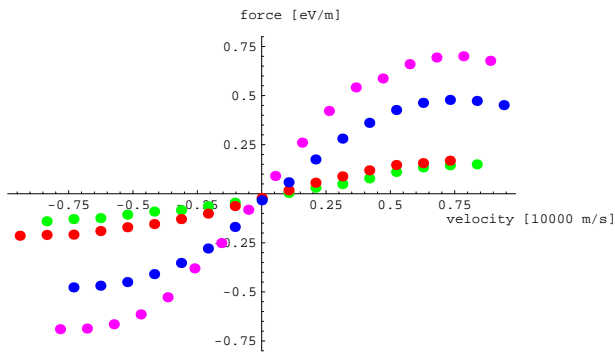


FIG. 4: Friction force for different magnetic fields with parameter $\alpha = 1.3$ (pink dots), 1.0 (blue), 0.9 (red), 0.8 (green).

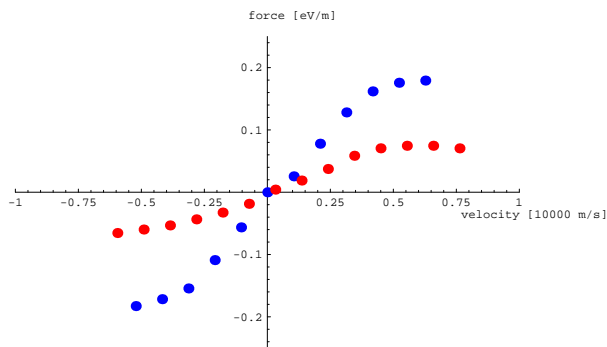


FIG. 5: Friction force with correctors on (blue dots, upper curve) and off (red dots) for $I_e = 100$ mA and $B = 0.06$ T.

In the fifth experiment we explore effects of solenoid errors. Most theoretical estimates do not take into account the effect of magnetic field errors. However, such errors can significantly decrease the strength of the force. This can be seen, for example, from Eq. 3, where such errors are included in a parametric fashion through Δ_{eff} . Larger Δ_{eff} moves the force maximum to a larger relative velocity reducing the force strength. The validity of

such a parametric description is not clear and requires detailed studies with numerical codes. The solenoid in the electron cooler in CELSIUS contains embedded correctors to straighten the magnetic field lines. Several measurements of the friction force curve and the corresponding Δ_{eff} were performed with the correctors switched on and off. The data are presently being compared with numerical results obtained using the VORPAL code [13], which simulates the friction force from first principles. An example of such measurement for an electron current of $I_e = 100$ mA is shown in Fig. 5 with the correctors switched on (blue dots) and off (red dots). The force is significantly reduced for larger perturbations of the magnetic field lines (correctors off).

To summarize, we have carried out a series of dedicated measurements of the longitudinal magnetized friction force aimed towards detailed benchmarking with theories and simulations. We also performed the measurements to address such issues as different degrees of magnetization and effects of solenoid imperfections, which are of critical importance for proposed high-energy cooling projects. Tens of the force curves were measured with good precision (see Table 1), and a raw data is available for direct validation of theoretical models. The force curves were measured for $B = 0.12$ T ($I_e = 500, 300, 100, 50$ mA), $B = 0.1$ T ($I_e = 500, 250, 100, 50, 20$ mA), $B = 0.08$ T ($I_e = 500, 300, 100$ mA), $B = 0.06$ T ($I_e = 500, 300, 100$ mA), $B = 0.05$ T ($I_e = 500, 300, 100$ mA), $B = 0.04$ T ($I_e = 500, 300$ mA), $B = 0.03$ T ($I_e = 300, 100, 50$ mA). To explore the dependence on the non-straightness of magnetic field lines, measurements were also done with correctors turned off for $I_e = 500$ mA ($B = 0.1, 0.04$ T), $I_e = 300$ mA ($B = 0.05, 0.04$ T), $I_e = 100$ mA ($B = 0.06, 0.03$ T). To explore the dependence on the tilt angle between the proton and electron beams, the force was measured for $B = 0.1$ T, $I_e = 250$ mA for the horizontal tilt angles of $\theta_x = 0, 0.2, 0.4, 0.8, -0.2, -0.4, -0.8$ mrad and for the angles in the vertical directions of $\theta_y = 0, 0.2, 0.4, 0.8, -0.2, -0.4, -0.8$ mrad. A systematic comparison of the data with theories requires detailed description of theoretical models and numerical simulations for each of the experiments, and will be presented in the future.

We would like to thank Dag Reistad and the The Svedberg Laboratory for providing beam time and support during these experiments. We thank Oliver Boine-Frankenheim and Ilan Ben-Zvi for taking an active role in planning of these experiments. A. Sidorin, A. Smirnov, and V. Ziemann acknowledge the support from INTAS grant 03-54-5584 "Advanced Beam Dynamics for Storage Rings". This work is supported by the US Department of Energy.

-
- [1] I. Meshkov, Nuc. Instr. Meth. **A 391**, 1 (1997).
- [2] H. Danared, Nuc. Instr. Meth. **A 391**, 24 (1997).
- [3] Y. Rao et al., Proc. of COOL01, Bad Honnef (2001).
- [4] T. Ellison, Proc. of 1991 Part. Accelerator Conf., p. 1612.
- [5] RHIC Ecooler, <http://www.agsrhichome.bnl.gov/eCool>
- [6] FAIR facility, <http://www.gsi.de/GSI-Future/cdr>
- [7] M. Sedláček et al., Proc. of Workshop on Cooling (Montreux, Switzerland, October 1993), CERN 94-03, 235.
- [8] D.D. Caussyn et al. Phys. Rev. **E 51**, 4947 (1995).
- [9] A. Burov, FERMILAB-TM-2213 (2003).
- [10] G. Parzen, Tech Note C-AD/AP/150 (2004).
- [11] A.V. Fedotov et al., Proc. of Particle Accelerator Conf. (Knoxville, TN, May 2005), TPAT091 (2005).
- [12] V. Parkhomchuk, Nuc. Instr. Meth. **A 441**, 9 (2000).
- [13] D.L. Bruhwiler et al., Proc. of Particle Accelerator Conf. (Knoxville, TN, May 2005), TPAT087 (2005).